Res. Rep. Fac. Eng. Mie Univ., Vol. 20, pp. 83-98(1995)

Original Paper

Creep Behavior of Concrete-Filled Steel Tubular Members

Chihaya YAMADA, Shosuke MORINO, Jun KAWAGUCHI and Toshiaki MACHIDA†
(Department of Architecture)

(Received September 18, 1995)

Abstract

In order to clarify the mechanical characteristics of concrete-filled steel square tubular (CFT) columns subjected to the long-term load, creep tests of CFT compression members and a CFT flexural member have been performed. The paper first presents the test results of the creep strain of the compression members, and compares them with the predictions by the analysis based on a visco-elastic model for a creeping material. The decrease in the concrete stress and the increase in the creep strain are clearly shown. Then, it shows the buckling analysis of slender CFT compression members, and discusses the reduction of the buckling strength due to the creep and the stress transfer behavior from the concrete to the steel tube. Finally, the test results of a CFT flexural member are presented with the analysis of the creep coefficient based on the age-adjusted equivalent coefficient method.

Key words

concrete-filled tube, creep, compression member, beam, buckling, creep coefficient

1. Introduction

It has been known that the creep effect under the long-term load must be considered to evaluate the deformation and the buckling strength of ordinary reinforced concrete beams and columns. However, it is not known whether or not a similar consideration is needed in the design of a concrete-filled steel tubular (abbreviated as CFT hereafter) member, since there have been very few

† Sato Kogyo Corporation

experimental work done in the past.

The creep effect of CFT members may be separated into two parts. The one is the reduction of Young's modulus of concrete, which is well known from the research of ordinary reinforced concrete members. The other is the stress transfer from concrete to steel tube, which may lead the steel stress into the inelastic range. These two types of creep effects are combined and cause the increase in displacement of a beam and the decrease in buckling strength of a compression member as the time passes. The paper deals with the experimental investigation on the creep behavior of CFT compression and flexural members subjected to the long-term loads in order to clarify the creep coefficient quantitatively, and with the buckling analysis of CFT compression members taking the creep effects into consideration.

2. Creep Behavior of CFT Compression Member

2.1 Experiment

The creep of CFT compression members was investigated under the log-term compression load, which were made of cold-formed square tube filled with concrete. The cross sections of tubes were □-100x100x3.2 and □-100x100x4.5, and the lengths were 40 and 80 *cm*. Total three specimens were prepared. Table 1 indicates the correspondence between the specimen name and

Table 1 List of specimens

Specimen name	Length (*mm*)	Tube thickness (*mm*)	Tube width (*mm*)
CR-40-4.5	396.0	4.36	100.12
CR-40-3.2	396.6	3.12	100.12
CR-80-3.2	796.5	3.12	99.96

Table 2 Material properties of steel tube

Tube section (STKR400)	Yield stress (N/mm^2)	Tensile strength (N/mm^2)	Young's modulus (kN/mm^2)	Elongation (%)
□-100×100×4.5	312.07	380.80	184.96	29.95
□-100×100×3.2	368.15	429.70	191.61	17.53

Table 3 Material properties of concrete

Age (day)	Compressive strength (N/mm^2)	Young's modulus (kN/mm^2)
28	13.57	17.12

experimental variables. Table 2 and 3 show the material properties of steel tube and concrete.

Figure 1 shows a test set-up. The specimen, together with a 20 *tonf* hydraulic jack and a load cell, was inserted into a loading apparatus consisting of two end-plates of 60 mm thick and 4 PC strands of diameter 12 *mm*. PC strands played a role of a spring to prevent too much load release due to the creep. Two sets of loading apparatus were prepared. Two specimens of length 40 *cm* connected together were testes in the one apparatus, and the specimen of length 80 *cm* in the other. A constant axial load of 103.9 *kN* was applied by the hydraulic jack, which was the average of the loads causing the stress in concrete equal to $F_c/3$ calculated for the 3 specimens based on Young modulus ratio of 10; F_c denotes the cylinder strength of concrete. Axial strains were measured by wire strain gauges mounted on the surface of the steel tube, every day before and after the axial load was adjusted to a prescribed value. The locations of gauges are shown in Fig. 2.

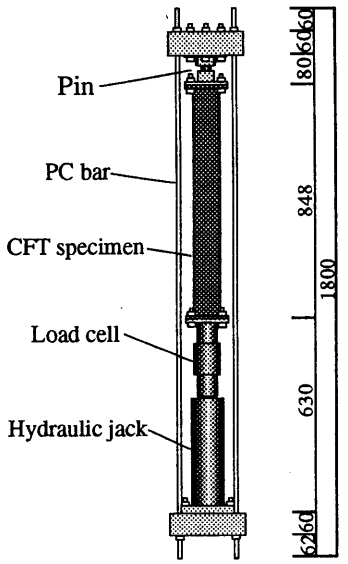

Fig. 1 Test set-up

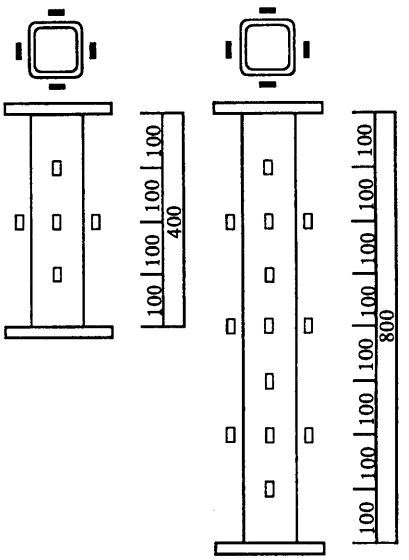

Fig. 2 Location of W.S.G.

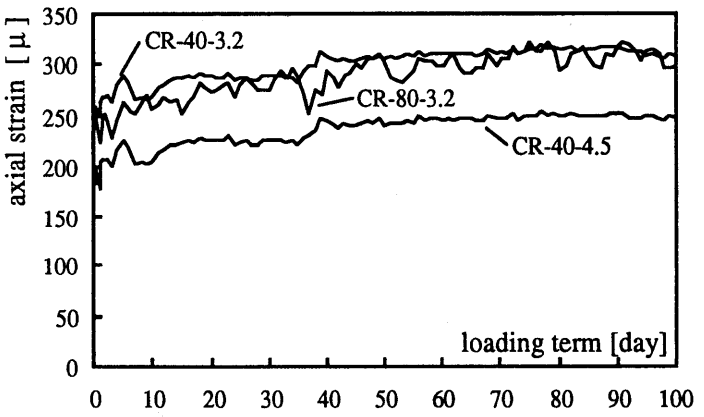

Fig. 3 Time-history of axial strains

2.2 Test results

The time-history of axial strains of 3 specimens are shown in Fig. 3. The specimens CR-40-3.2 and CR-80-3.2 having the same wall thickness of tube show very similar behavior, and thus the length of compression member may not affect the creep behavior. Figure 4 shows the time-history

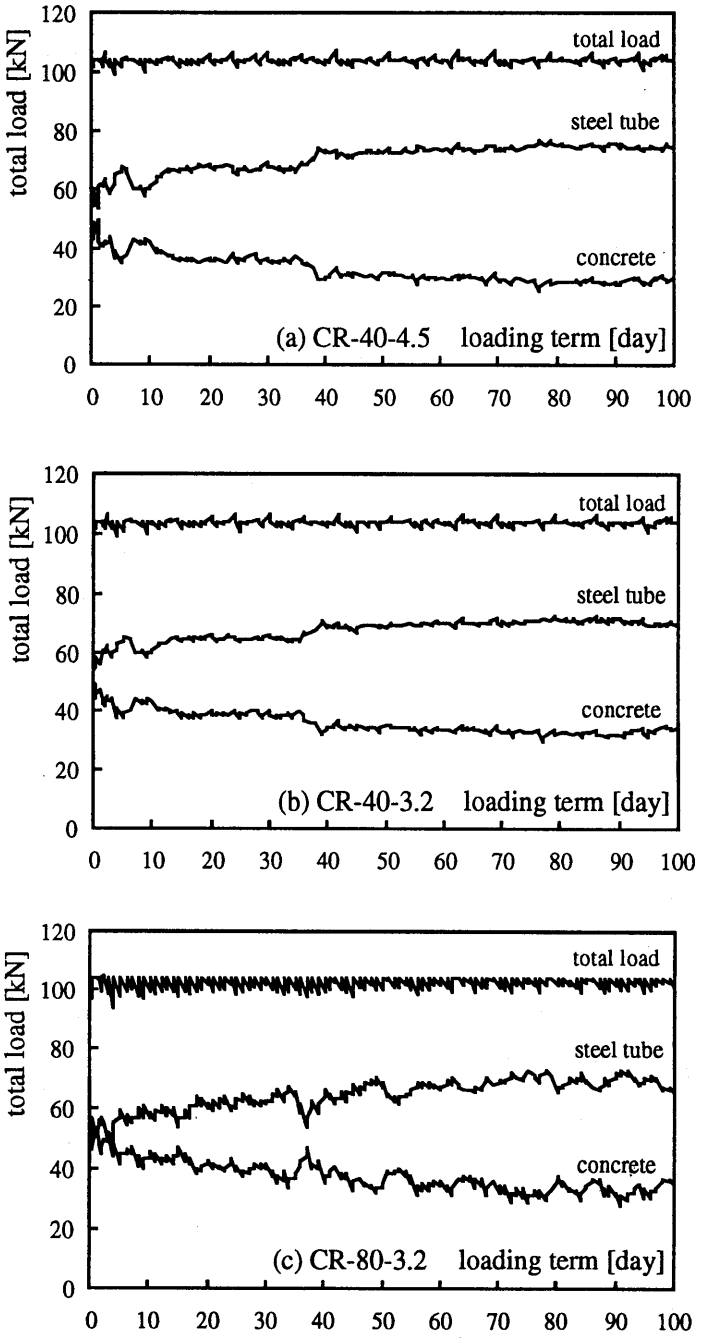

Fig. 4 Time-history of axial loads

of axial loads carried by concrete and steel tube together with the total applied load measured by the load cell. Notches appearing on the line for total load are due to the measurements taken before and after the axial load was adjusted to a prescribed value. The load carried by the steel tube is calculated from the measured data of the axial strain, and this is subtracted from the total load to obtain the load carried by the concrete. It is observed that the more load is carried by the steel tube with time due to the creep.

2.3 Analysis of creep coefficient

The time-history of creep strain is analyzed by the procedure shown in *Ref.* [1], which assums a visco-elastic model to express the stress-strain relations of a creeping material. First, the time-history of concrete stress may be expressed by

$$\sigma_c(t) = \sigma_0 \{\alpha + (1-\alpha) e^{-\gamma t}\} = \sigma_0 \psi(t) \tag{1}$$

where $\sigma_c(t)$ denotes the concrete stress which is a function of the time t (*day*), σ_0 the instantaneous concrete stress right after the application of axial load, and constants α and γ were determined by the curve-fitting from the experimental data. Figure 5 compares the test results with the curves given by *Eq.* (1) with the values of α and γ listed in Table 4. The data of concrete stress were obtained by dividing the load data of concrete shown in Fig. 4 by the concrete area. *Equation* (1) very well fits the test data.

The visco-elastic model is expressed by

$$\eta \dot{\varepsilon}(t) + E_c \varepsilon(t) = \sigma_c(t) \tag{2}$$

where $\varepsilon(t)$ and $\dot{\varepsilon}(t)$ denote concrete strain and its rate, respectively, E_c Young's modulus of concrete, and η coefficient of viscosity. The effect of shrinkage is not considered. Substituting *Eq.* (1) into *Eq.* (2) leads to a differential equation

$$\eta \dot{\varepsilon}(t) + E_c \varepsilon(t) - \sigma_0 \psi(t) = 0 \tag{3}$$

The solution is given as

$$\varepsilon(t) = \frac{\sigma_0}{E_c} \left\{ 1 + \alpha \left(1 - e^{-\beta t}\right) + (1-\alpha)\left(e^{-\gamma t} - e^{-\beta t}\right) / \left(1 - \frac{\gamma}{\beta}\right) \right\} \tag{4}$$

where $\beta = E_c/\eta$. Subtracting instantaneous strain σ_0/E_c from *Eq.* (4) leads to the expression for the creep strain ε_{cr}, as follows:

Table 4 Values of material constants

Specimen name	α	γ	E_c (kN/mm^2)	η (kN · day/mm^2)	β (day^{-1})
CR-40-4.5	0.54	0.0265	17.12	1740.2	0.0098
CR-40-3.2	0.6	0.0237	17.12	2177.9	0.0079
CR-80-3.2	0.6	0.0192	17.12	2601.3	0.0066

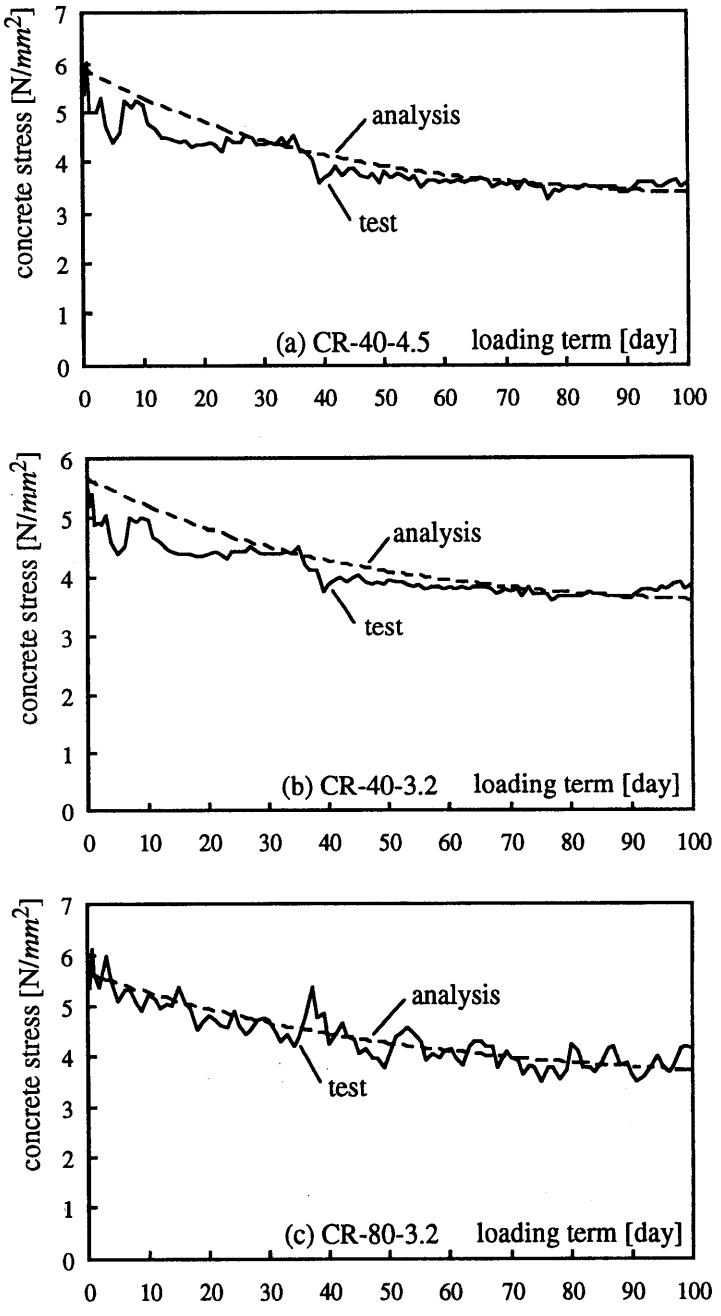

Fig. 5 Reduction of concrete stress

$$\varepsilon_{cr}(t)=\frac{\sigma_0}{E_c}\left\{\alpha\left(1-e^{-\beta t}\right)+(1-\alpha)\left(e^{-\gamma t}-e^{-\beta t}\right)/\left(1-\frac{\gamma}{\beta}\right)\right\} \tag{5}$$

The value of η which best fitted the test data was sought. The comparison between the time-history of creep strain ε_{cr} obtained from the test and *Eq.* (5) is shown in Fig. 6. The values of E_c and η listed in Tables 4 are used for the calculation of ε_{cr} by *Eq.* (5). *Equation* (5) well estimates the test

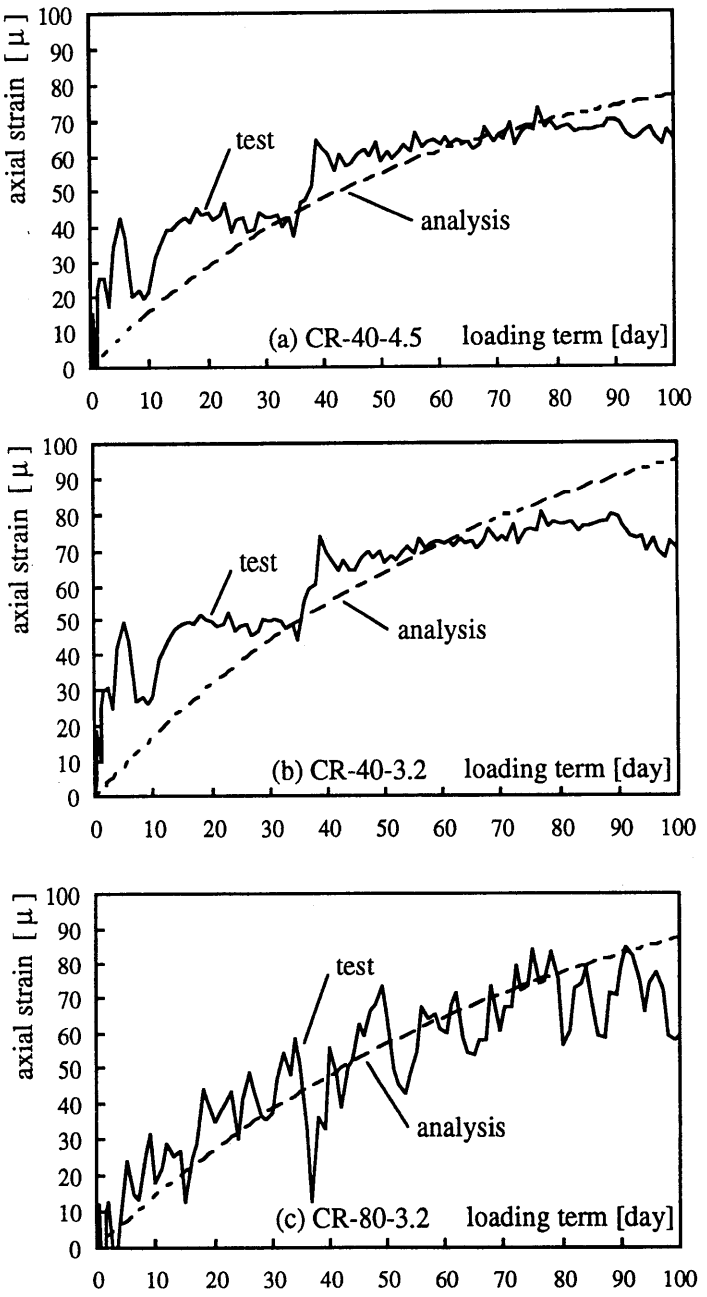

Fig. 6 Time-history of creep strains

results, but shows a tendency to overestimate the creep strain as the day proceeds. *Equation* (4) can be written in the form of

$$\varepsilon(t) = \frac{\sigma_0}{E_c}\{1 + \phi(t)\} \tag{6}$$

which indicates that Young's modulus of concrete E_c is reduced to $E_c/\{1 + \phi(t)\}$. The value of $\phi(t)$ is plotted for the case of CR-40-4.5 in Fig. 7.

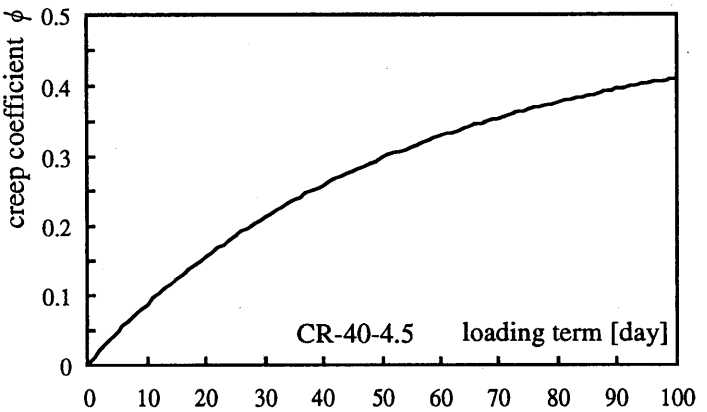

Fig. 7 Creep coefficient ϕ

3. Buckling Analysis of CFT Compression Member Affected by Creep

3.1 Model for analysis

Buckling analysis is performed for a model of a CFT compression member of length l subjected to a compression load P, which consists of a steel tube □-100x100x4.5 and filled concrete. Table 5 shows material properties and the values of parameters appearing in *Eq.* (4), which are assigned to the model. It is assumed that the concrete follows the relation between strain ε and time t (*day*) as given by *Eq.* (4), and the relation between stress σ and strain ε as given by *Eq.* (2). The steel tube is assumed to follow the stress-strain relation given as

$$\begin{aligned} &\text{when} \quad \sigma_s(t) \le 0.5\,\sigma_y; \quad \sigma_s(t) = E_s\,\varepsilon(t) \quad \text{or} \quad \varepsilon(t) = \frac{\sigma_s(t)}{E_s} \\ &\text{when} \quad \sigma_s(t) > 0.5\,\sigma_y; \quad \sigma_s(t) = \sigma_y\left\{1 - \frac{0.25\,\varepsilon_y}{\varepsilon(t)}\right\} \quad \text{or} \quad \varepsilon(t) = \frac{0.25\,\varepsilon_y}{1 - \sigma_s(t)/\sigma_y} \end{aligned} \tag{7}$$

where σ_s denotes steel stress which is a function of time t (*day*), σ_y yield stress of steel, E_s Young's

modulus of steel, and $\varepsilon_y = \sigma_y/E_s$. In the stress-strain relation above, the proportional limit stress is taken equal to 0.5 σ_y, and a hyperbolic type curve is used to express the relation in the inelastic range. The tangent modulus E_t is derived from *Eq.* (7) as follows:

$$\begin{aligned} &\text{when} \quad \sigma_S(t) \le 0.5\,\sigma_y; \quad E_t = E_S \\ &\text{when} \quad \sigma_S(t) > 0.5\,\sigma_y; \quad E_t = 4\,E_S\left(1 - \sigma_S(t)/\sigma_y\right)^2 \end{aligned} \tag{8}$$

Table 5 Values of material constants for analysis

Specimen name	α	γ	E_c [kN/mm^2]	η [kN · day/mm^2]	E_s [kN/mm^2]	σ_y [N/mm^2]
CR-40-4.5	0.54	0.0265	17.12	1740.2	184.96	312.07

3.2 Buckling analysis

The nominal value of Young's modulus of concrete t days after the application of a constant axial compression load, reduced due to the creep, is given by $E_c/\{1 + \phi(t)\}$, according to *Eq.* (6), and the flexural rigidity EI of a CFT member is given as follows:

$$EI = (EI)s + (EI)c = E_t I_S + E_C I_C \tag{9}$$

where I_s and I_c denote the second moments of inertia of steel and concrete cross sections, respectively. Then, the buckling strength of a CFT compression member t days after the application of compression load is given by

$$P_{cr}(t) = \frac{\pi^2 EI}{l^2} = \frac{\pi^2}{l^2}\{E_t I_S + E_C I_C\} \tag{10}$$

On the other hand, the buckling strength can be expressed by the stress generated in steel and concrete cross sections, as follows:

$$P_{cr}(t) = A_S\,\sigma_S(t) + A_C\,\sigma_C(t) \tag{11}$$

where A_s and A_c denote the cross-sectional areas of steel and concrete sections, respectively. Suppose now that the steel stress reaches to $\sigma_s(t)$ at t days and the buckling of the CFT member of length l occurs, then the strain $\varepsilon(t)$ in the CFT member can be determined from *Eq.* (7). Based on the assumption that the plane remains plane after the deformation takes place, the instantaneous concrete stress σ_0 is determined from *Eq.* (4) and the value of $\varepsilon(t)$, and then the concrete stress $\sigma_c(t)$ is

determined from *Eq.* (1). The value of $\phi(t)$ is independently determined from *Eq.* (6). The buckling strength $P_{cr}(t)$ is then determined from *Eq.* (11), and finally substituting the value of $P_{cr}(t)$ into *Eq.* (10) leads to the determination of member length l.

3.3 Results of analysis

When the day t at which the buckling occurs is assigned, the column buckling curve can be drawn by repeating the procedure explained above to determine the member length l for a given value of the steel stress $\sigma_s(t)$. Figure 8 shows several column curves for assigned days of the buckling occurrence. In the ordinate, P_{cr} is non-dimensionalized by $A_s\sigma_y$, and λ_s in the abscissa denotes the normalized slenderness ratio of steel tube and equal to $(l/i_s)(\sqrt{\varepsilon_y}/\pi)$, where i_s denotes the radius of gyration of steel section. Each curve consists of two parts; the one is for the buckling occurring in the inelastic range of the steel, and the other is for the elastic buckling, both curves showing hyperbolic shapes. Since it is assumed that the concrete is elastic, and the contribution of the concrete to the total load carrying capacity is large, the shape of the curve for the inelastic range of steel becomes similar to the curve for the elastic buckling. Dashed line indicates the point on the column curve at which the buckling occurs with the concrete strain equal the value shown. In the range of small slenderness ratio, the concrete stress goes up very high (when ε becomes 0.5 %, σ_c becomes 85.6 N/mm^2), and the curve in this range is unrealistic. It is observed from the column curve that when the buckling occurs more than 50 days after the application of the load, the creep shows rather small effect on the buckling strength, and almost no effect on the column buckling curve in the elastic range.

Figure 9 shows the change in the buckling strength and the steel stress with the time t (*day*) for the compression members with l/D = 15 and 30, where D denotes the width of square steel tube.

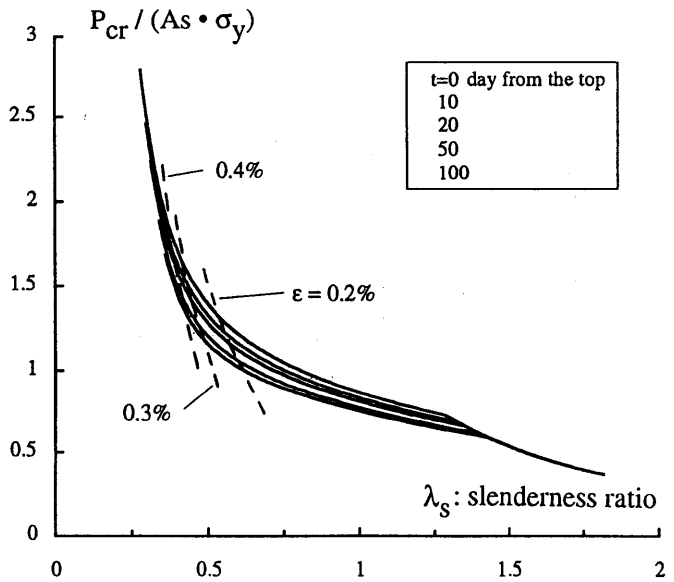

Fig. 8 Colum buckling curves

Chain line and dashed line indicate the buckling strength $P_{cr}/A_s\sigma_y$ and the steel stress σ_s/σ_y of the compression member which buckles t days after the application of the load, respectively. On the other hand, solid line indicates the change in the steel stress of the compression member subjected to the buckling load which is calculated on the assumption that the buckling occurs 50 (or 100) days after the application of the load. Solid line thus intersects with the dashed line at the day of 50 (or 100). It is observed from Fig. 9 that the buckling load (chain line) does not vary much in the region of more than 50 days, the curve of the steel stress is very flat and the change is small (dashed line), and the slope of the solid line is steeper in the shorter member, but the difference in the curve for the buckling occurrence at 50 days and 100 days is rather small.

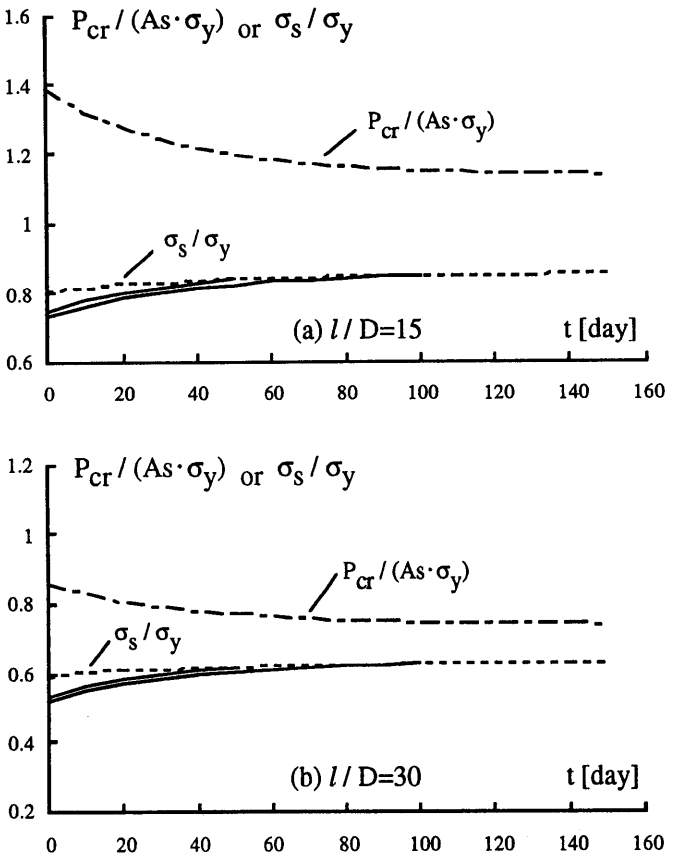

Fig. 9 Change in buckling strength and steel stresses

4. Creep Behavior of CFT Flexural Member

4.1 Experiment

The creep of a CFT flexural member was investigated under long-term flexural load. The cross section of a cold-formed square tube was □-100x100x3.2. Dimensions of a beam specimen

and mechanical properties of steel and concrete are shown in Tables 6 and 7, respectively. The specimen of length 300 *cm* was simply supported with the span of 260 *cm*, and two concentrated lateral loads were applied by weights at the location 95 *cm* apart from the supports, as shown in Fig. 10. The weight of 1077.6 *kg* caused the concrete stress nearly equal to the half the design standard strength of 20.6 N/mm^2. Measured every day were the displacement at the mid-point of the specimen relative to the supports, and the longitudinal strains on the upper and lower surfaces of steel tube at 5 locations; mid-point and points 15 and 30 *cm* apart from the mid-point.

Table 6 Dimensions of specimen

Specimen name	Span length (*mm*)	Tube thickness (*mm*)	Tube width (*mm*)
BR-260-3.2	2600	3.02	99.98

Table 7 Material properties of steel and concrete

Steel tube				Concrete
Yield stress (N/mm^2)	Tensile strength (N/mm^2)	Young's modulus (kN/mm^2)	Elongation (%)	Compressive strength (N/mm^2) [Age:28days]
426.95	494.57	195.15	15.5	24.39

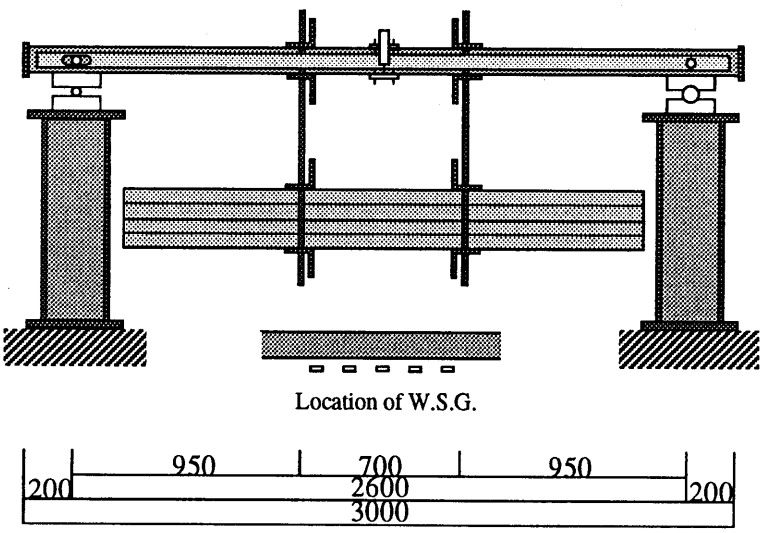

Fig. 10 Test set-up

4.2 Test results

Figure 11 shows the time-history of longitudinal strains at the tension and the compression extreme fibers obtained from 5 wire strain gauges. The creep strains at the compression fibers are

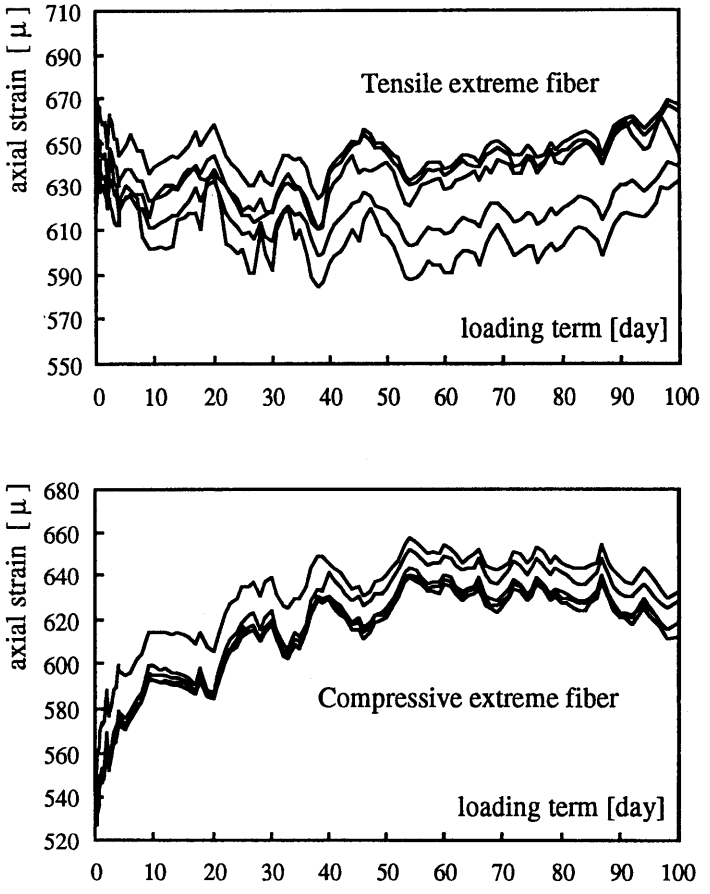

Fig. 11 Time-history of steel strains

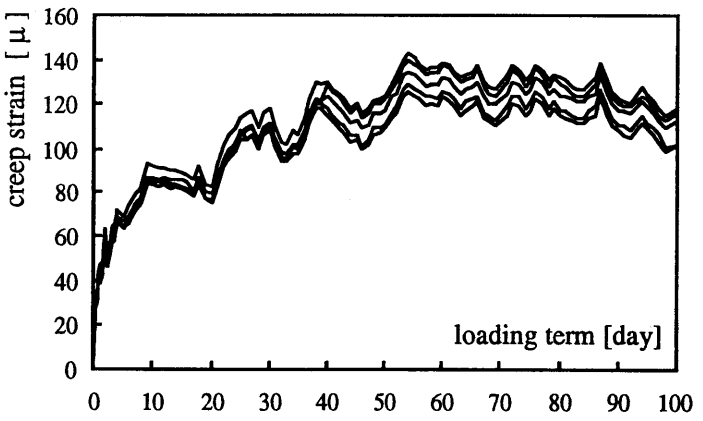

Fig. 12 Time-history of creep strains in compression

shown in Fig. 12. Note that the tensile strains gradually decrease while the compressive strains increase, which indicates that the location of neutral axis moves down as the time passes. The time-history of displacement at the mid-point of the beam is shown in Fig. 13, where a gradual increase is observed.

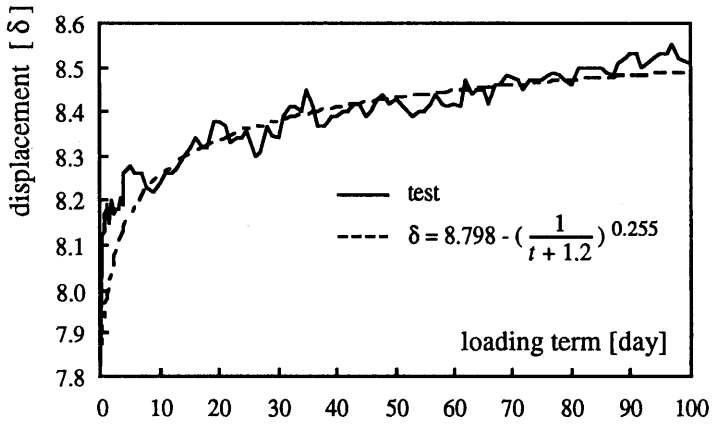

Fig. 13 Time-history of mid-point displacement

4.3 Analysis of creep coefficient

There have been no information about the creep coefficient of a CFT flexural member, and thus it is analyzed by the age-adjusted effective modulus method [2], based on the following mathematical expression of the time-history curve of the mid-point displacement shown in Fig. 13,

$$\delta = 8.798 - \left(\frac{1}{t+1.2}\right)^{0.255} \tag{12}$$

which was determined by the least square fitting to the experimental data. Suppose that the strain distribution t days after the application of the load is given as shown by the white triangles in Fig. 14 (a), and the strain and tcurvature increase due to the creep by the next day by the amount of $\varepsilon\phi$ and $\kappa\phi$, without changing the location of the neutral axis k_0, as shown by the hatched triangles in Fig. 14 (a), where ϕ denotes the creep coefficient. According to the strain change, the stress change $E_s\varepsilon\phi$ in the steel and $E_c\varepsilon\phi/(1+\phi)$ in the concrete are generated in the cross section, and the stresses are not in the equilibrium. Unbalanced bending moment ΔM and axial thrust ΔN are generated. The negative value of these unbalanced resultant forces are applied to the cross section, as shown in Fig. 14 (c), in order to fulfill the equilibrium condition, and the stress and strain distributions are analyzed, which are superposed on the corresponding stress and strain distributions shown in Fig. 14 (a) and (b), to obtain the solution for the $(t+1)th$ day. The neutral axis which is newly determined shifts down as shown in Fig. 14 (d). In this analysis, it is assumed that the linear relation holds between the stress and the strain after the creep occurring, thus the principle of

superposition holds, Young's modulus of concrete is reduced by the ratio of $1/(1 + \phi)$, and the tension stress in concrete is ignored. The effect of shrinkage of concrete is ignored.

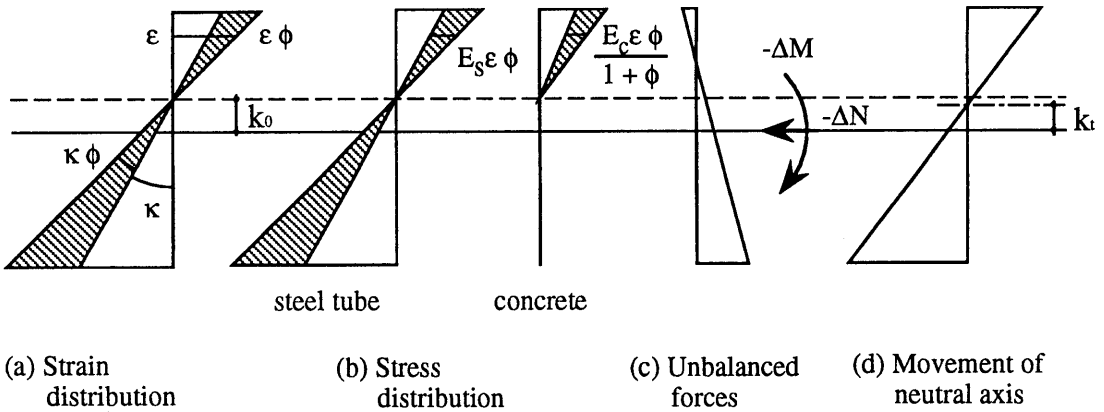

Fig. 14 Strain and stress distributions in cross section

Once the curvature distribution is determined from the procedure above, the displacement is obtained by the Mohr's principle as a function of ϕ. The value of ϕ at the day t is determined by equating the displacement theoretically determined in the present analysis to the test data, and the results are shown in Fig. 15. It is observed from the figure that the value of ϕ at t = 100 days is about 0.08 which is much smaller than the value for an ordinary reinforced concrete beam.

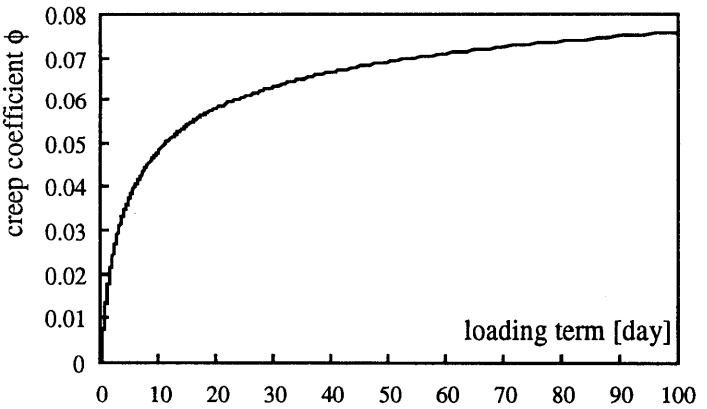

Fig. 15 Creep coefficient ϕ

5. Conclusions

Creep tests of CFT compression and flexural members and the buckling analysis of CFT compression members affected by the creep were performed, and the following observations were made.

Tests of CFT compression members:

1) The amount of axial creep strain is not affected by the length of specimen.

2) The time-history of creep strain can be traced by the analysis based on the visco-elastic model given by *Eqs.* (1) through (5).

3) The value of creep coefficient ϕ obtained by the analysis is much smaller than that indicated for an ordinary reinforced concrete member in the literature.

Buckling analysis of CFT compression members:

4) The buckling strength calculated on the assumption that the buckling occurs t days after the application of the load does not vary much if the day t is set more than 50 days.

5) The amount of axial stress carried by the steel tube does not vary much regardless of the day of the buckling occurrence.

Test of a CFT flexural member:

6) The extreme fiber strains in tension and compression measured at the surface of the steel tube gradually decrease and increase, respectively, and the neutral axis shifts down, as the time passes, due to the creep.

7) The value of creep coefficient ϕ obtained by the analysis based on the age-adjusted effective modulus method is much smaller than that for an ordinary reinforced concrete beam.

References

[1] Ichinose, L. H., A. Kurita and H. Nakai: *An experimental Study on Creep of Concrete-Filled Steel Pipes*, Proc. 3rd International Conference on Steel and Concrete Composite Structures, Fukuoka, Japan, pp. 55 - 60, 1991.9.

[2] Gilbert, R. I.: *Time Effects in Concrete Structures*, Elssevier, p. 91, 1988.